

Characteristics and Performance of the CCD Photometric System at Lulin Observatory

Daisuke Kinoshita^{1,2}, Chin-Wei Chen¹, Hung-Chin Lin¹, Zhong-Yi Lin¹,
Kui-Yun Huang¹, Yung-Shin Chang¹ and Wen-Ping Chen¹

¹ Institute of Astronomy, National Central University, 300 Jungda Rd, Jungli City, Taoyuan, 320-54, Taiwan; kinoshita@astro.ncu.edu.tw

² National Astronomical Observatory of Japan, 2-21-1 Osawa, Mitaka, Tokyo, 181-8588, Japan

Received 2004 September 1; accepted 2005 March 11

Abstract The Lulin One-meter Telescope at Lulin Observatory in Taiwan started open-use observations in January 2003. In order to evaluate the performance of the CCD photometric system, the characteristics and quality of the site, we obtained data of photometric standards as well as calibration data from February to November 2004. We report here the results of our analysis including the gain, readout noise, dark current and linearity of the CCD camera, and transformation coefficients, total throughputs, night sky brightnesses and limiting magnitudes for *UBVRI* bands.

Key words: instrumentation: miscellaneous — site testing — telescopes

1 INTRODUCTION

The Lulin One-meter Telescope (hereafter, LOT) was installed in September 2002 on the summit of Mount Lulin (120°52'25" E, 23°28'7" N, $H = 2862$ m) in central Taiwan by the Institute of Astronomy of National Central University. After three months of test observations, the open-use observations began in January 2003 (Chang 2004). It is essential to know the properties and performance of the instrument to conduct scientific observations. We have started a program to evaluate the characteristics of the CCD photometric system on LOT in November 2003. Here, we report the results of our analysis of the performance of the CCD photometric system and the characteristics and qualities of the site. We briefly introduce the instrument in Sect. 2, report on the basic characteristics of the CCD in Sect. 3, give the transformation coefficients in Sect. 4, and show the total system performances in Sect. 5, and summarize in Sect. 6.

2 INSTRUMENT

LOT has an effective diameter of 1000 mm. The CCD imaging camera is attached to the Cassegrain focus of the telescope. In June 2003, the CCD camera “VersArray:1300B” man-

ufactured by Princeton Instruments, Inc. started operation. The specifications of the camera are available from Princeton Instruments, Inc. (www.princetoninstruments.com). Table 1 lists some of its essential parameters. The telescope focal length is 8000 mm, resulting in a pixel scale of 0.516 arcsec per pixel. This is reasonably spatially sampled under the typical seeing of 1.8 arcsec at Lulin Observatory. The field of view of this system is 11.5 arcmin by 11.2 arcmin. The CCD is cooled by thermoelectric cooling aided by water circulation. The typical operation temperature is -50°C . Acquisition of the CCD image is done using the software “Maxim DL” provided by the Diffraction Limited, Inc. running on Windows operating system.

Table 1 Specifications of the CCD camera VersArray:1300B as provided from Roper Scientific, Inc.

CCD Chip	EEV CCD36-40 (back-side illuminated)
Pixel Number	1340×1300
Pixel Size	$20 \mu\text{m} \times 20 \mu\text{m}$
Imaging Area	$26.8 \text{ mm} \times 26.0 \text{ mm}$
AD Conversion	16 bits
Sampling	50 kHz (slow mode), 1 MHz (fast mode)

3 PERFORMANCE OF THE CCD

3.1 Bias

The mean bias level is about 89 ADU (Analog-to-Digital Unit) for the slow readout mode, and about 150 ADU for the fast readout mode. The readout time of the fast readout mode is less than 2 seconds, and the efficiency of data acquisition is very high. This mode is powerful especially for taking flatfields during the twilight. Figures 1 and 2 show the stability of mean bias levels for the slow and fast readout modes, respectively. It seems the mean bias level of the fast readout mode is correlated with the ambient temperature, and changes more than 15 ADU within a day. One explanation is stray light causing an increase of the bias level after sunrise in the morning. However, the stray light cannot explain the gradual decrease at night. The control software of the CCD stores the temperature reading of the CCD at the beginning of the exposure. It shows a constant temperature even when the ambient temperature changes. The amplifier may be affected by the ambient environment, and we need further investigations of this phenomenon. Because of this instability, the observer is advised to take frequent bias frames during the night for high precision photometry when the fast readout mode is used.

3.2 Gain and Readout Noise

The gain G is the factor that converts the digital output to the number of electrons:

$$n_e = G n_{\text{ADU}}. \quad (1)$$

Here, n_e is the number of electrons, n_{ADU} is the Analog-to-Digital Unit (ADU), and G (e^-/ADU) is the gain. The standard deviation of the difference between two flatfield images $\sigma_{F_1-F_2}$ contains Poisson noise in addition to the readout noise (Howell 2000),

$$\sigma_{F_1-F_2}^2 = 2 \left\{ \left(\frac{\sqrt{n_e}}{G} \right)^2 + \left(\frac{R}{G} \right)^2 \right\}. \quad (2)$$

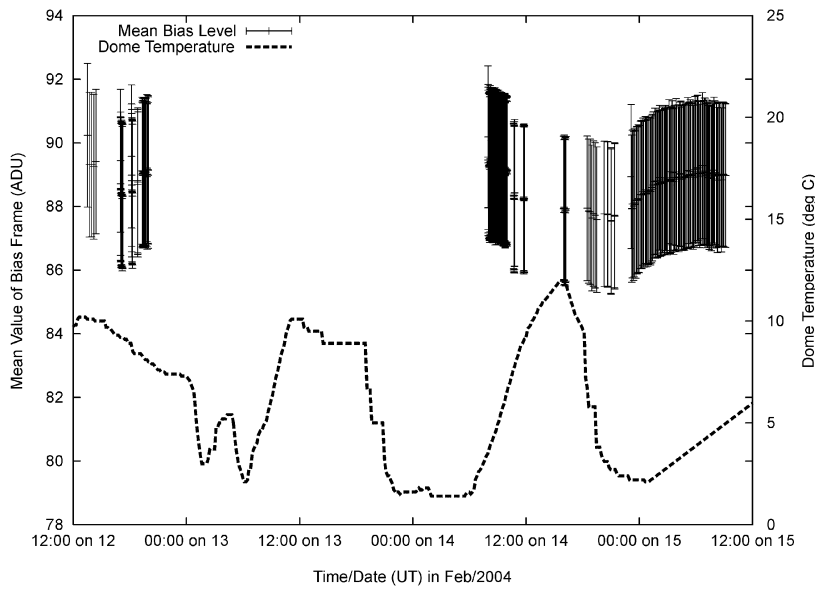


Fig. 1 Level of bias frame, plotted against data acquisition time in UT. The data are taken in the slow readout mode.

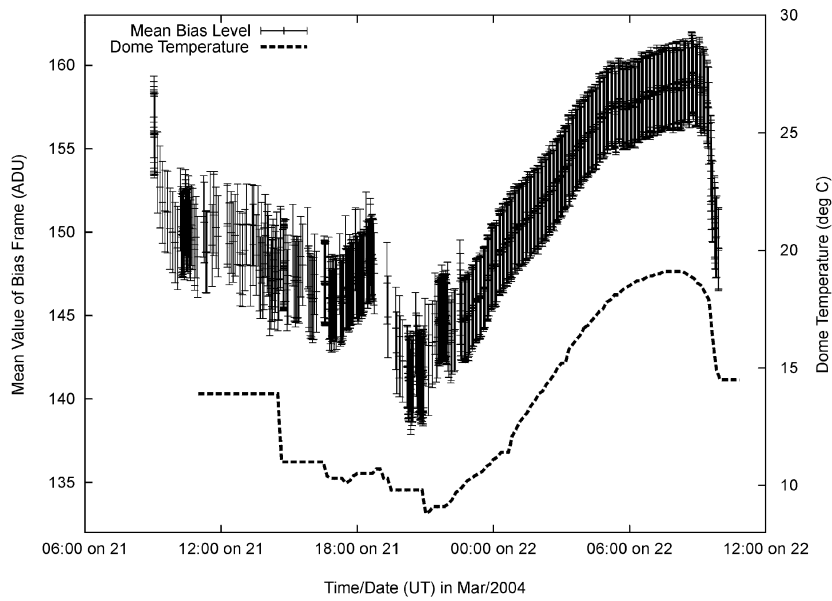


Fig. 2 Level of bias frame, plotted against data acquisition time in UT. The data are taken in the fast readout mode. The ambient temperature in the dome of the LOT is shown as the dotted line.

Here, R (e^-) is the readout noise. Subtracting two flatfield images increases the noise by a factor of $\sqrt{2}$. Hence, the correlation between the signal S and the noise N is expressed as

$$N = \sqrt{\frac{S}{G} + \left(\frac{R}{G}\right)^2}. \quad (3)$$

We took flatfield images using a white screen in the dome. We used both broad- and narrow-band filters to cover a wide range of signal levels. We used B for the broad-band filter and CN for the narrow-band filter. The integration times were set from 3 to 60 s. For each integration time, five frames were continuously taken. We tested both the fast readout mode of 1 MHz sampling and slow readout mode of 50 kHz sampling. Basically we followed the method described by Motohara et al. (2002). All the measurements were carried out under a cooling temperature of -50°C . Since we took five frames for each signal level, we made 10 pairs of two frames from five frames. For each pair of images, we subtracted one from the other, and measured the standard deviation. We divided the standard deviation by $\sqrt{2}$ to derive the noise level. We also subtracted combined dark frame from flatfield images to measure the mean signal level of the flatfields to derive the signal level. To check the uniformity of the properties of the CCD, we divided the CCD into four regions. Here, we call the $301 \leq x \leq 600$, $301 \leq y \leq 600$ region of the image “Region A”, $301 \leq x \leq 600$, $701 \leq y \leq 1000$ “Region B”, $701 \leq x \leq 1000$, $301 \leq y \leq 600$ “Region C”, and $701 \leq x \leq 1000$, $701 \leq y \leq 1000$ “Region D”. The signal and the noise were measured for all four regions.

The results of the measurements for the fast and slow readout modes are shown in Figs. 3 and 4, respectively. We fitted the measurements with Eq. (3). The gain G is $3.0 e^-/\text{ADU}$ for all four regions for fast readout mode, and is $2.0e^-/\text{ADU}$ for all four regions for slow readout mode. The readout noise is $7.1\text{--}7.4e^-$ for fast readout mode, and $4.4\text{--}4.5e^-$ for slow readout mode.

3.3 Dark Current

Dark frames with different integration times were obtained to estimate the dark current generation rate. Results are summarized in Table 2. The average value shows $0.064e^- \text{ s}^{-1} \text{ pix}^{-1}$ for the operation temperature of -50°C .

3.4 Linearity

In order to check the linearity of the response of the CCD, we carried out measurement using a camera lens and LEDs. We placed eight LEDs in a sphere. We attached the camera lens to the CCD and located the CCD at the small hole of the sphere. We imaged inside of the sphere for various exposure time ranging 5 to 80 s. For each exposure time, we took five frames. The measurements were done using slow readout mode, and the dark component was subtracted. Figure 5 shows the mean count of 100×100 pixels near the center of the field against exposure time. We fitted the data with the formula

$$C = at^\gamma + b. \quad (4)$$

Here, C is the mean count, t is the exposure time, a , b and γ are constants. The deviation from $\gamma = 1$ is 0.1% for 3000 to 38 000 ADU. The non-linearity becomes to 1.7% when the mean count reaches 51 000 counts.

4 PHOTOMETRIC CALIBRATIONS

In order to compare results of photometry with those from other instruments, one needs to convert the magnitudes from the instrumental system into the standard system. To achieve this

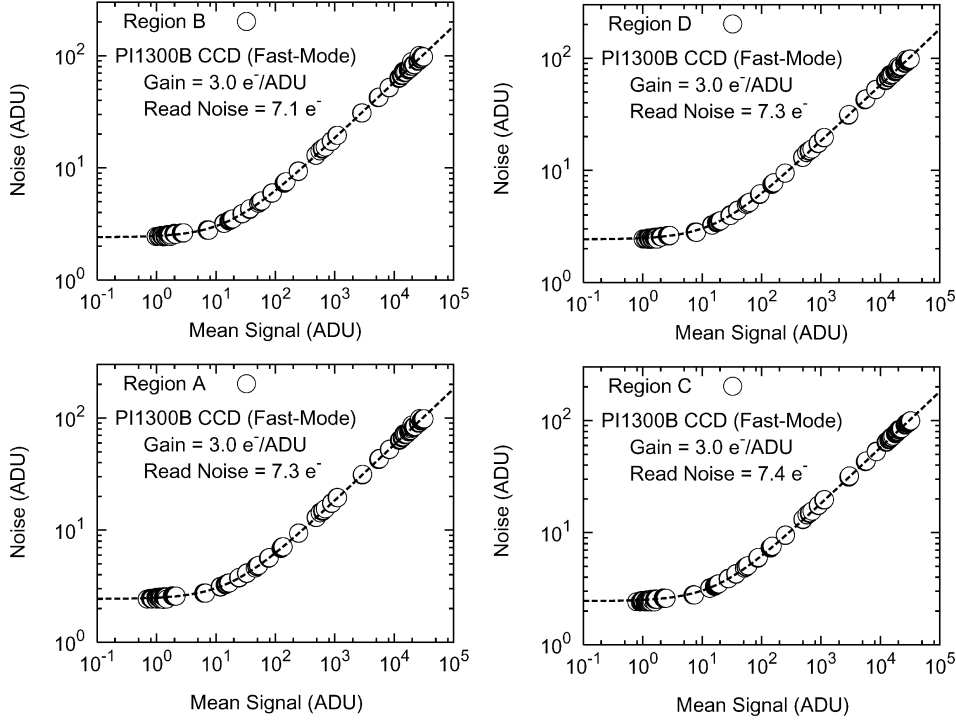


Fig. 3 Signal and the noise of 300×300 regions on the CCD for fast readout mode. The dotted curves are the fit using Eq. (3).

conversion, it is essential to evaluate the transformation coefficients. Here, we define transformation equations as

$$U_{\text{std}} = U_{\text{inst}} + Z_U - \{k'_U + k''_U(U - B)\}X + C_U(U - B), \quad (5)$$

$$B_{\text{std}} = B_{\text{inst}} + Z_B - \{k'_B + k''_B(B - V)\}X + C_B(B - V), \quad (6)$$

$$V_{\text{std}} = V_{\text{inst}} + Z_V - \{k'_V + k''_V(B - V)\}X + C_V(B - V), \quad (7)$$

$$R_{\text{std}} = R_{\text{inst}} + Z_R - \{k'_R + k''_R(V - R)\}X + C_R(V - R), \quad (8)$$

$$I_{\text{std}} = I_{\text{inst}} + Z_I - \{k'_I + k''_I(V - I)\}X + C_I(V - I), \quad (9)$$

where $U_{\text{std}}, B_{\text{std}}, V_{\text{std}}, R_{\text{std}}, I_{\text{std}}$ are the standard magnitudes, $U_{\text{inst}}, B_{\text{inst}}, V_{\text{inst}}, R_{\text{inst}}, I_{\text{inst}}$ are the instrumental magnitudes, Z_U, Z_B, Z_V, Z_R, Z_I are zero point magnitudes, $k'_U, k'_B, k'_V, k'_R, k'_I$ are the first-order extinction coefficients, $k''_U, k''_B, k''_V, k''_R, k''_I$ are the second-order extinction coefficients, C_U, C_B, C_V, C_R, C_I are the color terms, and X is the airmass. The net fluxes inside the aperture for standard stars are normalized to the exposure time of 1 s when calculating the instrumental magnitudes. We have chosen photometric standards from the list provided by Landolt (1992) to cover a wide range of colors and airmass. We have used $UBVRI$ filters. The $BVRI$ filters are based on the Bessell system, and their transmission properties are reported by Huang et al. (2004). The property of the U -band filter is unknown and we are planning to measure the transmittance in the laboratory. Basically we used the “photcal” package of IRAF (Image Reduction and Analysis Facility, provided and maintained by NOAO) to fit the data and derive the coefficients. The values are confirmed by manual analysis using the method described

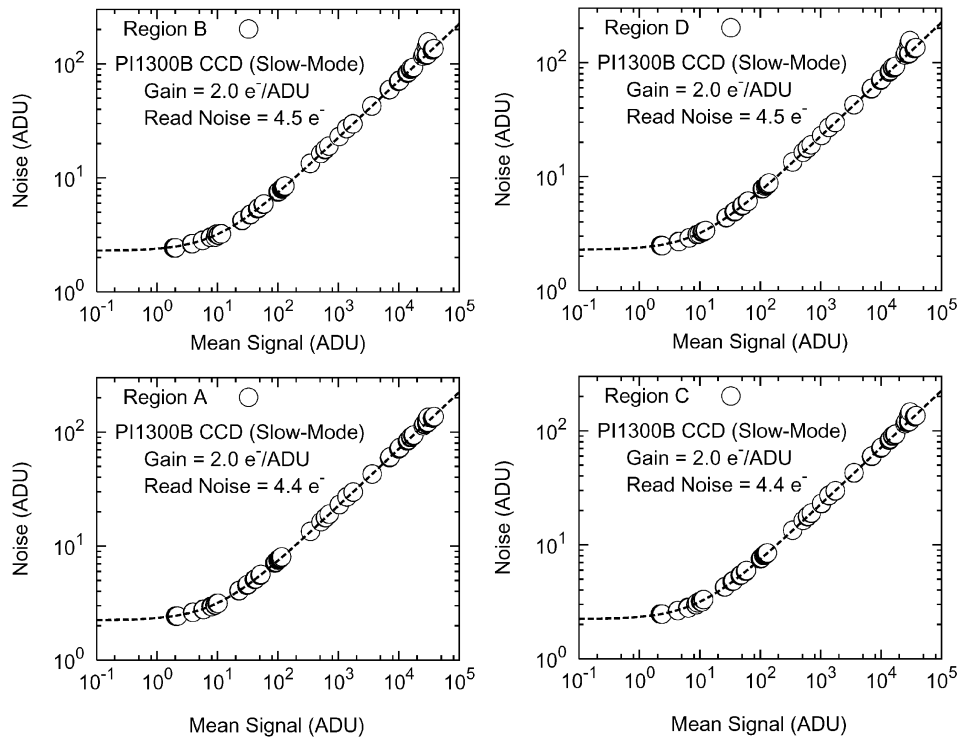


Fig. 4 Signal and the noise of 300×300 regions on the CCD for slow readout mode. Dotted curves are the fit using Eq. (3).

Table 2 The dark current generation rates. The second column shows the readout mode. The word “slow” denotes 50 kHz sampling, and “fast” denotes 1 MHz sampling. The third column shows the operating temperature of the CCD. The dark current generation rate is expressed in number of electrons per second per pixel.

Date	Readout	Temp. ($^{\circ}\text{C}$)	Dark Current ($\text{e}^{-1} \text{s}^{-1} \text{pix}^{-1}$)
13/Feb/2004	fast	-50	0.063
24/May/2004	slow	-50	0.067
25/May/2004	fast	-50	0.065
26/May/2004	fast	-50	0.055
22/Jun/2004	slow	-50	0.065
23/Jun/2004	slow	-50	0.073
24/Jun/2004	slow	-50	0.065
25/Jun/2004	slow	-50	0.057
16/Aug/2004	slow	-50	0.059
17/Aug/2004	slow	-50	0.070

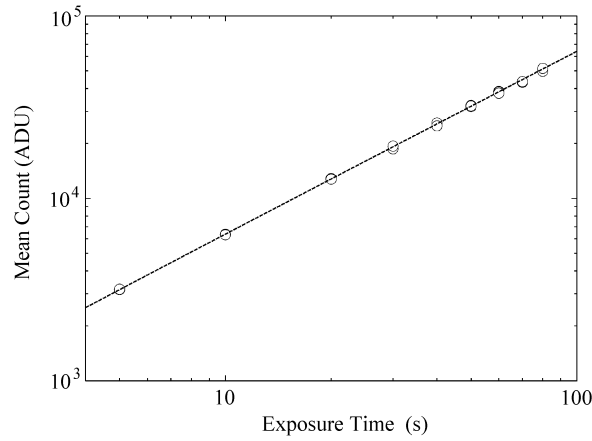


Fig. 5 A plot of the exposure time versus mean count of the CCD. The light source is eight LEDs. The dotted line is the fit using Eq. (4).

by Henden & Kaitchuck (1990). The second-order extinction terms are found to be small and we ignored them. The results for seven different nights are summarized in Table 3. The sky was photometric and stable on these seven nights. The plots of the Landolt magnitude versus calculated magnitude using derived transformation coefficients on 25 June, 2004 are shown in Fig. 6. No systematic errors are recognized. The atmospheric extinction coefficients at various astronomical sites are summarized in Table 4. The extinction coefficients at Lulin Observatory on relatively dry nights are comparable to those of major ground based observatories.

The instrumental colors are plotted against Landolt standard colors in Fig. 7. The linear fits give the following relations,

$$(U - B) = 1.18(u - b) - 3.02, \quad (10)$$

$$(B - V) = 1.25(b - v) - 0.41, \quad (11)$$

$$(V - R) = 0.99(v - r) + 0.03, \quad (12)$$

$$(V - I) = 0.91(v - i) + 0.64, \quad (13)$$

$$(R - I) = 0.82(r - i) + 0.57. \quad (14)$$

Here, capital letters refer to the standard system and small letters, the instrumental system.

5 SYSTEM PERFORMANCE

5.1 System Efficiency

Using the photometric observations of the Landolt standard fields, we have estimated the total throughput of the telescope and instrument including telescope optics, filter transmittance and detector quantum efficiency.

The energy coming into the circle of diameter D outside the Earth's atmosphere from a star of magnitude m_λ per second is expressed as

$$E_\lambda = F_\lambda 10^{-0.4m_\lambda} \pi \left(\frac{D}{2} \right)^2 \Delta\lambda. \quad (15)$$

Table 3 Transformation coefficients including zero point magnitudes, first order extinction coefficients, and color terms of LOT plus VersArray:1300B for *UBVRI* filters on seven different nights. The extinction coefficients are in units of magnitude per airmass. On 17 Feb 2004, the fast readout mode was used, and the zero point magnitudes are different from other nights. For other six nights, the slow readout mode was used.

	17/Feb/2004	19/Apr	24/Jun	25/Jun	01/Sep	09/Nov	11/Nov/2004
Z_U	20.02 ± 0.03	20.20 ± 0.10	20.23 ± 0.05	20.28 ± 0.06			
Z_B	22.34 ± 0.02	22.83 ± 0.01	22.82 ± 0.02	22.81 ± 0.02	22.76 ± 0.08	22.70 ± 0.01	22.78 ± 0.01
Z_V	22.68 ± 0.02	23.11 ± 0.01	23.11 ± 0.02	23.11 ± 0.01	23.06 ± 0.05	23.01 ± 0.01	23.09 ± 0.03
Z_R	22.66 ± 0.01	23.07 ± 0.04	23.08 ± 0.02	23.10 ± 0.02	23.00 ± 0.02	22.96 ± 0.01	23.05 ± 0.02
Z_I	21.99 ± 0.04		22.36 ± 0.03	22.43 ± 0.03	22.40 ± 0.03	22.30 ± 0.02	22.37 ± 0.04
k_U	0.45 ± 0.01	0.46 ± 0.01	0.41 ± 0.02	0.41 ± 0.03			
k_B	0.19 ± 0.02	0.25 ± 0.01	0.24 ± 0.01	0.21 ± 0.01	0.22 ± 0.04	0.21 ± 0.01	0.20 ± 0.01
k_V	0.11 ± 0.01	0.16 ± 0.01	0.16 ± 0.01	0.13 ± 0.01	0.10 ± 0.02	0.12 ± 0.01	0.12 ± 0.01
k_R	0.09 ± 0.01	0.12 ± 0.01	0.13 ± 0.01	0.11 ± 0.01	0.05 ± 0.01	0.08 ± 0.01	0.09 ± 0.01
k_I	0.06 ± 0.01		0.08 ± 0.03	0.08 ± 0.02	0.10 ± 0.02	0.06 ± 0.01	0.04 ± 0.01
C_U	$+0.15 \pm 0.02$	$+0.30 \pm 0.10$	$+0.32 \pm 0.02$	$+0.32 \pm 0.06$			
C_B	$+0.20 \pm 0.02$	$+0.14 \pm 0.01$	$+0.15 \pm 0.01$	$+0.11 \pm 0.02$	$+0.21 \pm 0.03$	$+0.17 \pm 0.01$	$+0.13 \pm 0.01$
C_V	-0.06 ± 0.02	-0.06 ± 0.01	-0.06 ± 0.01	-0.08 ± 0.02	-0.05 ± 0.02	-0.07 ± 0.01	-0.10 ± 0.03
C_R	-0.05 ± 0.02	-0.12 ± 0.05	-0.07 ± 0.02	-0.15 ± 0.03	-0.13 ± 0.01	-0.12 ± 0.02	-0.12 ± 0.02
C_I	$+0.04 \pm 0.03$		$+0.05 \pm 0.01$	$+0.04 \pm 0.03$	$+0.07 \pm 0.01$	$+0.03 \pm 0.03$	$+0.00 \pm 0.03$

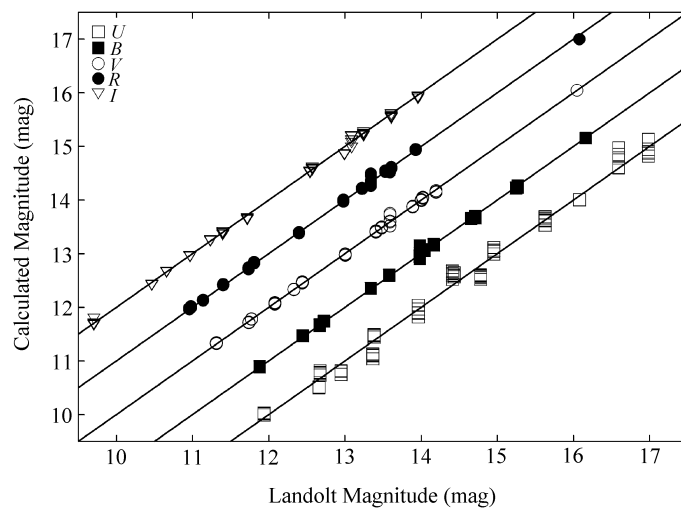


Fig. 6 Landolt magnitude versus calculated magnitude using derived transformation coefficients for *UBVRI*. The data taken on 25 June, 2004 are used for the plot. The *U*, *B*, *R*, *I* calculated magnitudes are shifted to -2 , -1 , $+1$, $+2$, respectively, to fit all the data into a single figure.

Table 4 Atmospheric extinction coefficients for selected ground based astronomical observatories. The first order extinction coefficients for *UBVRI* bands are shown in units of mag per unit airmass. The numbers in the parenthesis are the errors.

Site	<i>U</i>	<i>B</i>	<i>V</i>	<i>R</i>	<i>I</i>	Ref.
Brooks	0.62(0.09)	0.37(0.07)	0.25(0.04)	0.20(0.06)	0.14(0.07)	Miller & Osborn, 1996
Gaomeigu			0.14			Tan & Zhang, 1999
Kiso		0.27(0.02)	0.17(0.01)	0.09(0.01)	0.05(0.01)	Ito, 1998a
Kitt Peak			0.20(0.01)		0.08(0.02)	French et al., 1985
La Palma			0.11			Guerrero et al., 1998
La Silla		0.25	0.13	0.07	0.03	Mattila et al., 1996
La Silla	0.46	0.23	0.12			Nakos et al., 1997
Lulin	0.43(0.02)	0.20(0.02)	0.12(0.01)	0.10(0.01)	0.07(0.02)	This work
Mauna Kea (2800-m)		0.31	0.18			Krisciunas et al., 1987
Mauna Kea (4200-m)		0.20	0.11			Krisciunas et al., 1987
Paranal	0.50(0.03)	0.26(0.01)	0.17(0.01)	0.13(0.01)	0.07(0.02)	Giacconi et al., 1999
Paranal	0.44(0.01)	0.23(0.01)	0.11(0.01)	0.07(0.01)	0.03(0.01)	Hanuschik, 2004
Siding Spring	0.54(0.02)	0.31(0.03)	0.16(0.03)	0.11(0.02)	0.09(0.03)	Sung & Bessell, 2000
Tololo	0.56	0.28	0.16	0.12		Stone & Baldwin, 1983
Xinglong	0.60	0.31	0.20	0.14	0.05	Yan et al., 2000

Here, F_λ is the flux of a 0 magnitude star at wavelength λ , and $\Delta\lambda$ is the half-width of the filter. The number of incoming photons N_{photon} are calculated as

$$N_{\text{calc}} = \frac{E_\lambda}{h\nu} = \frac{E_\lambda\lambda}{hc}. \tag{16}$$

Here, h is the Planck constant and c is the the light speed. The extinction corrected count rate of the CCD N_{obs} is expressed as

$$N_{\text{obs}} = \frac{C_{\text{raw}}}{T_{\text{exp}}} 10^{-0.4kX} G. \tag{17}$$

Here, C_{raw} is the integrated raw count of the star, T_{exp} is the exposure time, k is the first-order extinction coefficient, X is the airmass, and G is the gain of the CCD. We define the total throughput E as

$$E = \frac{N_{\text{obs}}}{N_{\text{calc}}}. \tag{18}$$

The results are summarized in Table 5. Since the transmittance of the *U*-band filter is unknown, we have assumed a typical value. Results for both the slow and fast readout modes have a good agreement.

5.2 Sky Background Brightness

The brightness of the night sky was measured using the data taken on 24, 25 June 2004. It was 6 and 7 days after the new moon, respectively. The Moon was almost going to set on 24 June, and the elevation was 4.0 to -0.5 degree above the horizon. On 25 June, the elevation of the Moon was 22.3 to 11.0 degree above the horizon. We selected 4-minute single exposures on 24 June and 5-minute single exposures on 25 June in each of the *UBVRI* bands. The angular separations between the moon and target field on 24 and 25 June were 65 and 53 degrees,

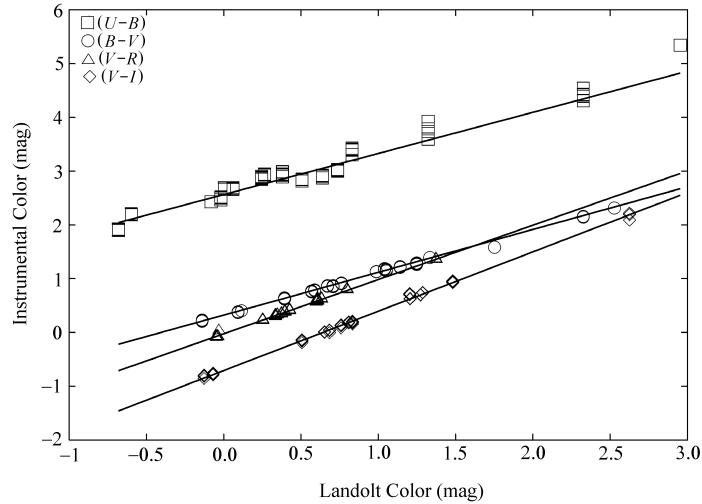


Fig. 7 Landolt standard colors and the extinction corrected instrumental colors are plotted for $(U - B)$, $(B - V)$, $(V - R)$ and $(V - I)$. The solid straight lines are the least-square fit of the data. The data were collected on 25 June, 2004.

Table 5 The total throughput for $UBVRI$ bands including telescope optics, filter transmittance and quantum efficiency of the detector. Since the transmittance of the U -band filter is unknown, we assumed a typical value.

Date	U	B	V	R	I	Remarks
17/Feb/2004	8%	27%	55%	47%	20%	fast readout
24/Jun/2004	7%	26%	53%	45%	19%	slow readout
25/Jun/2004	6%	27%	54%	47%	20%	slow readout

respectively. The airmasses were 1.17 to 1.26 on 24 June, and 1.13 to 1.22 on 25 June. The correction for the airmass was applied using the formula (Krisciunas & Schaefer 1991)

$$B_0(Z) = B_{\text{zen}} 10^{-0.4k(x-1)x}, \quad (19)$$

where

$$x = (1 - 0.96 \sin^2 Z)^{-0.5}. \quad (20)$$

Here, $B_0(Z)$ is the night sky brightness at zenith distance Z , B_{zen} is the night sky brightness at zenith, k is the extinction coefficient. We measured the mean background level using the software “source extractor”. The derived instrumental magnitudes and colors were converted into the standard system using the coefficients in Table 3. The color terms are taken into account. The background brightness levels of $UBVRI$ bands on 24 June, 2004 are $U = 21.78 \pm 0.30$, $B = 22.01 \pm 0.08$, $V = 21.28 \pm 0.06$, $R = 20.91 \pm 0.05$, and $I = 19.40 \pm 0.06$ mag arcsec $^{-2}$, respectively. On 25 June 2004, they were $U = 21.03 \pm 0.20$, $B = 21.22 \pm 0.06$, $V = 20.83 \pm 0.04$, $R = 20.59 \pm 0.05$, and $I = 19.47 \pm 0.05$ mag arcsec $^{-2}$, respectively. The values we obtained at Lulin were compared to those of major ground based astronomical observatories in Table 6.

Although the night sky brightnesses for B and V -band are roughly 0.8 and 0.5 magnitude brighter than the major astronomical sites, they seem to be typical in East Asian region. Lulin appears dark toward longer wavelengths, in the R and I bands. Lin (1994) reported the dark time night sky brightness at Lulin as $B = 21.22$ and $V = 20.72$ mag arcsec⁻² which are brighter than reported in this work. Lin used a 35-cm telescope with a focal reducer and a commercial CCD camera ST-6. The resulting pixel scale was 2.4×2.8 arcsec, which is larger than typical seeing size at Lulin. Faint stars or galaxies might have been included in the “sky” measurements. Also, the observations were carried out at airmass of 1.13–1.14, the correction for airmass was not applied. Taking into these factors, we believe the results from Lin (1994) and ours are mutually consistent.

Table 6 The dark time night sky brightness for $UBVRI$ bands measured at major ground based observatories. The brightness of the night sky is expressed in the unit of mag arcsec⁻².

Site	U	B	V	R	I	Ref.
Calar Alto	22.2	22.6	21.5	20.6	18.7	Leinert et al., 1995
Kiso		22.1	21.2	19.9	18.7	Ito, 1998b
Kitt Peak		22.9	21.9			Pilachowski et al., 1989
La Palma	22.0	22.7	21.9	21.0	20.0	Benn & Ellison, 1998
La Silla		22.8	21.7	20.8	19.5	Mattila et al., 1996
Lulin	21.8	22.0	21.3	20.9	19.5	This work
Mauna Kea		22.8	21.9			Krisciunas, 1997
Paranal	22.3	22.6	21.6	20.9	19.7	Patat, 2003
Tololo	22.0	22.7	21.8	20.9	19.9	Walker, 1987
Xinglong			21.0			Liu et al., 2003

5.3 Limiting Magnitude

We estimated the limiting magnitudes of LOT and PI1300B photometric system at Lulin. We used readout noise, dark current generation rate and sky background brightness estimated in this work. Derived limiting magnitudes for slow readout mode are $U = 19.7$, $B = 21.4$, $V = 21.2$, $R = 21.1$, and $I = 19.9$ mag for a signal-to-noise ratio of 10 with an integration time of 300s and an aperture size of 3 arcsec.

6 SUMMARY

The performance of the LOT and VersArray:1300B CCD photometric system at Lulin Observatory in Taiwan was evaluated. We have found variability in the bias level when the fast-readout mode is used. The gain of the CCD is different for slow and fast readout. The transformation coefficients and the relation of instrumental and standard colors are derived. The extinction coefficients at Lulin on relatively dry nights are comparable to major astronomical sites. The total system performance was also measured. The night sky brightness seems to be typical of observatories in the East Asia region.

Acknowledgements We would like to express our hearty thanks to Mr. Shih Jun-Shiung, Mr. Du Jing-Chuan, Mr. Shih Hao-Wei, and Mr. Wan Zong-Jing for their local supports at Lulin Observatory. We also thank Mr. Chang Ming-Shin, Mr. Urata Yuji, Miss Li Yang-Shyang for their help with the observations. Kinoshita, D. thanks to the fellowship from the Japan Society for Promotion of Science (ID: 15-1-2-02681-1).

References

- Benn D. R., Ellison S. L., 1998, *New Astronomy Reviews*, 42, 503
Chang M.-S., 2004, In: Chang M.-S. ed., *Annual Report of Lulin Observatory*, (in Chinese), p.14
French L. M. et al., 1985, *AJ*, 90, 668
Giacconi R. et al., 1999, *A&A*, 343, L1
Guerrero M. A. et al., 1998, *New Astronomy Reviews*, 42, 529
Hanuschik R., 2004, www.eso.org/observing/dfo/quality
Henden A. A., Kaitchuck R. H., 1990, *Willmann-Bell, Inc., Astronomical Photometry* (ISBN 0-943396-25-5), p.322
Howell S. B., 2000, *Handbook of CCD Astronomy* (ISBN 0-521-64834-3), Cambridge University Press
Huang Y.-J., Lee C.-C., Chen W.-P., 2004, In: Chang M.-S. ed., *Annual Report of Lulin Observatory*, (in Chinese), p.47
Ito N., 1998a, "*Observation of Photometric Standard Stars*" in the Internal Report of Kiso Observatory (in Japanese)
Ito N., 1998b, "*Estimation of the Limiting Magnitude of 2KCCD Camera*" in the Internal Report of Kiso Observatory (in Japanese)
Krisciunas K., Schaefer B., 1991, *PASP*, 103, 1033
Krisciunas K., 1997, *PASP*, 109, 1181
Krisciunas K., Sinton W., Tholen K. et al., 1987, *PASP*, 99, 887
Landolt A. U., 1992, *AJ*, 104, 372
Leinert C., Vaisanen P., Mattila K., Lehtinen K., 1995, *A&AS*, 112, 99
Lin H.-C., 1994, *Measurements of Night Sky Brightness using Open Cluster M44 at Lulin Observatory*, master thesis at National Central University of Taiwan (in Chinese)
Liu Y., Zhou X., Sun W. H. et al., 2003, *PASP*, 115, 495
Mattila K., Vaisanen, P., Appen-Schnur, G. F. O. V., 1996, *A&AS*, 119, 153
Miller R., Osborn W., 1996, *IAPPP Communications*, 63, 40
Motohara K., Iwamuro F., Maihara T. et al., 2002, *PASJ*, 54, 315
Nakos T., Sinachopoulos D., van Dessel E., 1997, *A&AS*, 124, 353
Patat F., 2003, *A&A*, 400, 1183
Pilachowski C. et al., 1989, *PASP*, 101, 707
Stone R. P. S., Baldwin, J. A., 1983, *MNRAS*, 204, 347
Sung H.-K., Bessell M. S., 2000, *PASA*, 17, 244
Tan H.-S., Zhang B.-R., 1999, In: Chen P.-S. ed., *The Proceedings of the 4th East Asian Meeting on Astronomy (4th EAMA), Observational Astrophysics in Asia and its Future*, p.18
Walker A., 1987, *NOAO Newsletter*, 10, 16
Yan H.-J. et al., 2000, *PASP*, 112, 691